Supplementary file:
Pertussis immunity and epidemiology:
mode and duration of vaccine-induced immunity

F.M.G. Magpantay[1], M. Domenech de Cellès[1],
P. Rohani[1,2,3] and A.A. King[1,2,3,4,5]

S1 Model equations

Here we present the stochastic and deterministic forms of the Full Model. The Restricted Models are easily derived from these by fixing the values of some of the vaccine parameters, as described in the text.

Stochastic model

The Full Model tracks the movement of individuals among eight compartments (vaccinated V, susceptibles S_1 and S_2, exposed E_1 and E_2, infected I_1 and I_2, and recovered R). The fluxes between compartments are illustrated in Figure 2 in the main text. The exposed and infected classes are further subdivided into subcompartments (E_1^k, E_2^k, I_1^k, I_2^k, for $k = 1, \ldots, K$). The stochastic model is a continuous-time, discrete state Markov process. Its state variables are the numbers of individuals in each of the aforementioned compartments. We let V denote the number in the V compartment; S_1, that in the S_1 compartment, and so on. We let $X = \left(V, S_1, S_2, E_1^1, \ldots, E_1^K, E_2^1, \ldots, E_2^K, I_1^1, \ldots, I_2^K, R\right)$ denote the vector of state variables. The process itself is most straightforwardly defined in terms of counting processes, i.e., non-negative, non-decreasing, integer valued processes. Let $Z_{AB}(t)$ denote the total number of individuals that have passed from compartment A to compartment B between time t_0 and time t, where t_0 is some arbitrary starting time prior to the first data point. We define the stochastic process in two steps. First, we specify the probability of every possible change in Z_{AB} for all A and B. Then, we describe how the state variables (the numbers of individuals in each compartment) depend on the counting processes, Z_{AB}.

The first step is accomplished by the following statements, where t is an arbitrary time, $h > 0$ is an arbitrary time increment, and $\Delta Z_{AB} = Z_{AB}(t+h) - Z_{AB}(t)$ is the change in the Z_{AB} counting

[1]Department of Ecology and Evolutionary Biology, University of Michigan, Ann Arbor, MI 48109, USA
[2]Center for the Study of Complex Systems, University of Michigan, Ann Arbor, MI 48109, USA
[3]Fogarty International Center, National Institutes of Health, Bethesda, MD 20892, USA
[4]Department of Mathematics, University of Michigan, Ann Arbor, MI 48109, USA
[5]To whom correspondence should be addressed.

process over the time interval $[t, t+h)$.

$$\begin{aligned}
\text{Prob}\left[\Delta Z_{VS_2} = 1 \mid X\right] &= \alpha\, V\, h + o(h) \\
\text{Prob}\left[\Delta Z_{VE_2} = 1 \mid X\right] &= \varepsilon_L\, \lambda\, V\, h + o(h) \\
\text{Prob}\left[\Delta Z_{S_i E_i^1} = 1 \mid X\right] &= \lambda\, S_i\, h + o(h) \\
\text{Prob}\left[\Delta Z_{E_i^{k-1} E_i^k} = 1 \mid X\right] &= K\, \sigma\, E_i^{k-1}\, h + o(h) \\
\text{Prob}\left[\Delta Z_{E_i^K I_i^1} = 1 \mid X\right] &= K\, \sigma\, E_i^K\, h + o(h) \\
\text{Prob}\left[\Delta Z_{I_i^{k-1} I_i^k} = 1 \mid X\right] &= K\, \gamma\, I_i^{k-1}\, h + o(h) \\
\text{Prob}\left[\Delta Z_{I_i^K R} = 1 \mid X\right] &= K\, \sigma\, I_i^K\, h + o(h)
\end{aligned} \tag{1}$$

where $i = 1, 2$ and $k = 2, \ldots, K$. In the above, λ is the force of infection with multiplicative noise, as discussed in the main text.

$$\lambda(t) = \left(\frac{\beta(t)(I_1 + \theta I_2) + \beta_1 \iota}{N(t)}\right) \Delta Q, \qquad \Delta Q \sim \text{Gamma}\left(\text{shape} = \frac{h}{\beta_{sd}^2}, \text{scale} = \frac{\beta_{sd}^2}{h}\right). \tag{2}$$

The mean transmission rate is given by the parameter β_1, the amplitude of seasonality by β_2 and the peak timing in transmission by φ,

$$\beta(t) = \beta_1(1 + \beta_2 \cos(2\pi(t - \varphi))). \tag{3}$$

In addition, all events of the form $\{\Delta Z_{AB} > 1 \mid X\}$ and $\{\Delta Z_{AB} > 0\ \&\ \Delta Z_{CD} > 0 \mid X\}$ for $(A, B) \neq (C, D)$ have probabilities that are $o(h)$. The changes in the sizes of the compartments and subcompartments over the $[t, t+h)$ interval obey the following equations.

$$\begin{aligned}
\Delta V &= (1 - \varepsilon_A) p\, \mu_B\, N - \Delta Z_{VS_2} - \Delta Z_{VE_2} \\
\Delta S_1 &= (1 - (1 - \varepsilon_A) p)\, \mu_B\, N - \Delta Z_{S_1 E_1} \\
\Delta E_1^1 &= \Delta Z_{S_1 E_1} - \Delta Z_{E_1^1 E_1^2} \\
\Delta E_1^k &= \Delta Z_{E_1^{k-1} E_1^k} - \Delta Z_{E_1^k E_1^{k+1}} \\
\Delta E_1^K &= \Delta Z_{E_1^{K-1} E_1^K} - \Delta Z_{E_1^K I_1^1} \\
\Delta I_1^1 &= \Delta Z_{E_1^K I_1} - \Delta Z_{I_1^1 I_1^2} \\
\Delta I_1^k &= \Delta Z_{I_1^{k-1} I_1^k} - \Delta Z_{I_1^k I_1^{k+1}} \\
\Delta I_1^K &= \Delta Z_{I_1^{K-1} I_1^K} - \Delta Z_{I_1^K R} \\
\Delta S_2 &= \Delta Z_{VS_2} - \Delta Z_{S_2 E_2} \\
\Delta E_2^1 &= \Delta Z_{VE_2^1} + \Delta Z_{S_2 E_2^1} - \Delta Z_{E_2^1 E_2^2} \\
\Delta E_2^k &= \Delta Z_{E_2^{k-1} E_2^k} - \Delta Z_{E_2^k E_2^{k+1}} \\
\Delta E_2^K &= \Delta Z_{E_2^{K-1} E_2^K} - \Delta Z_{E_2^K I_2^1} \\
\Delta I_2^1 &= \Delta Z_{E_2^K I_2^1} - \Delta Z_{I_2^1 I_2^2} \\
\Delta I_2^k &= \Delta Z_{I_2^{k-1} I_2^k} - \Delta Z_{I_2^k I_2^{k+1}} \\
\Delta I_2^K &= \Delta Z_{I_2^{K-1} I_2^K} - \Delta Z_{I_2^K R} \\
\Delta R &= \Delta Z_{I_1^K R} + \Delta Z_{I_2^K R},
\end{aligned} \tag{4}$$

where $k = 2, \ldots, K-1$. In the above, N denotes the total population size, μ_B the birth rate, and p the vaccination coverage. In this paper, we have taken $K = 3$.

Numerically, the stochastic process above is simulated using a multinomial version of the tau-leap algorithm (He *et al.*, 2010). To ensure that the simulations maintain the observed rate of population growth, at each time step all compartments and subcompartments X_j are adjusted to reflect the death rate (μ) and immigration rate (r). This is done via,

$$X_j \leftarrow \left[X_j e^{-(\mu+r)\Delta t}\right], \tag{5}$$

were $[\cdot]$ stands for the operation of rounding to the nearest integer value.

Simulations were performed using a stepsize of $h = 0.01$ yr, equal to 3.65 da. Such a stepsize has the effect of distorting the latent and infectious periods. Using the discrete time formula in He *et al.* (2010), the effective of latent period is lengthened from 8 da to 9.96 da, and the infectious period from 14 da to 15.9 da.

The time-varying birth (μ_B), death (μ), and immigration rates (r) for each region were calculated from EuroStat (European Commission, 2014) annual data on number of births, deaths and population sizes. Throughout a simulation, the population sizes were calculated using log-linear interpolation of the annual values, and the corresponding birth and death rates were calculated using linear interpolation. The model was initialized in 1994 to coincide with the estimated start of vaccination with aP. The vaccine coverage (p) from 1994–2000 were approximated by a linear function starting at a vaccination rate of 30% in 1994 (based on information on national vaccination averages) and the region-specific levels registered in the 2001 vaccine coverage data. The annual vaccine coverage values from 2001–2010 were linearly interpolated from the available data (Ministero della Salute, 2014).

Deterministic model

Taking expectations of the stochastic model in (1)–(5), taking the limit as $h \downarrow 0$ yields the following system of differential equations.

$$
\begin{aligned}
\frac{dV}{dt} &= (1-\varepsilon_A)p\,\mu_B\,N - \alpha V - \varepsilon_L \lambda V - (\mu + r)V,\\
\frac{dS_1}{dt} &= (1-(1-\varepsilon_A)p)\,\mu_B\,N - \lambda S_1 - (\mu + r)S_1,\\
\frac{dE_1^1}{dt} &= \lambda S_1 - K\sigma E_1^1 - (\mu + r)E_1^1,\\
\frac{dE_1^k}{dt} &= K\sigma E_1^{k-1} - K\sigma E_1^k - (\mu + r)E_1^k,\\
\frac{dE_1^K}{dt} &= K\sigma E_1^{K-1} - K\sigma E_1^K - (\mu + r)E_1^K,\\
\frac{dI_1^1}{dt} &= K\sigma E_1^K - K\gamma I_1^1 - (\mu + r)I_1^1,\\
\frac{dI_1^k}{dt} &= K\gamma I_1^{k-1} - K\gamma I_1^k - (\mu + r)I_1^k,\\
\frac{dI_1^K}{dt} &= K\gamma I_1^{K-1} - K\gamma I_1^K - (\mu + r)I_1^K,\\
\frac{dS_2}{dt} &= \alpha V - \lambda S_2 - (\mu + r)S_2,\\
\frac{dE_2^1}{dt} &= \varepsilon_L \lambda V + \lambda S_2 - \sigma E_2 - (\mu + r)E_2,\\
\frac{dE_2^k}{dt} &= K\sigma E_2^{k-1} - K\sigma E_2^k - (\mu + r)E_2^k,\\
\frac{dE_2^K}{dt} &= K\sigma E_2^{K-1} - K\sigma E_2^K - (\mu + r)E_2^K,\\
\frac{dI_2^1}{dt} &= K\sigma E_2 - \gamma I_2 - (\mu + r)I_2,\\
\frac{dI_2^k}{dt} &= K\gamma I_2^{k-1} - K\gamma I_2^k - (\mu + r)I_2^k,\\
\frac{dI_2^K}{dt} &= K\gamma I_2^{K-1} - K\gamma I_2^K - (\mu + r)I_2^K,\\
\frac{dR}{dt} &= K\gamma I_1^K + K\gamma I_2^K - (\mu + r)R.
\end{aligned}
\tag{6}
$$

These equations can be solved using a discretization similar to that used in the stochastic system. This is done by setting $\beta_{sd} = 0$, and taking the transitions at each step to be equal to the rates from (1) times h. Changes in the values of the components were then calculated using (4), and the sizes of each component were rescaled according to (5). Thus, the deterministic form of the model is the skeleton of the stochastic model minus the environmental stochasticity (stemming from β_{sd}) and demographic stochasticity (from the multinomial draws). It also experiences the same distortion in the latent and infectious period due to the choice of stepsize.

S2 Profiling

One dimensional likelihood profiles provide the values of the best likelihoods that can be obtained at fixed values of the *profile parameter* by maximizing over all the remaining model parameters. For each region, we started the profiling procedure by dividing the profile parameter's given range into equally spaced intervals (using a linear scale for β and ι and a logarithmic scale for all other parameters). For each interval, we gathered all the points from earlier searches (i.e. points from the initial search and those from prior profiling procedures) where the profile parameter had values that fell within the interval, and selected the point with the highest likelihood. This yielded an initial profile. To refine the profile, we created seven copies of the the initial and perturbed the values of the profile parameter by multiplying it by $0.95^3, 0.95^2, 0.95, 1.00, 1.05, 1.05^2$ and 1.05^3. These provided the starting point for profiling, i.e. maximizing the likelihood over the remaining model parameters. This procedure of generating starting points then profiling was iterated at least two times for each profile parameter, and at least three times for each vaccine parameter. The procedure was stopped when the points in the profile appeared to be converging to a curve.

The six regions were assumed to have independent dynamics. Once all profiles appear to have converged for each of the six regions, aggregated profiles were generated using the following procedure: A profile was generated for each region using 100 equally spaced intervals (in the linear or logarithmic scale) over the entire allowable range of each profile parameter, and selecting the points with the highest likelihood whose profile parameter falls within each interval. A function was then fit through this collection of points using local regression. This function was used to estimate the likelihood values at 101 equally spaced fixed points (the endpoints of the 100 intervals), for each region. The aggregated profile could then be calculated by adding the estimated log-likelihoods at each fixed point and fitting a function through those points.

S3 Akaike Information Criterion

The AIC with small sample size correction is given by the formula below,

$$\mathrm{AIC}_c = \underbrace{-2\,\log(\text{Likelihood}) + 2K}_{\text{AIC}} \quad + \quad \underbrace{\frac{2K(K+1)}{n-K-1}}_{\text{small sample correction}}, \tag{7}$$

where n is the number of data points and K is the number of parameters in a model (Burnham & Anderson, 2002).

S4 Relative infectiousness and relative reporting probability

In most of the individual regions, the results of profiling over the vaccine parameters independently support a high relative infectiousness ($\theta \to 1$) and low relative reporting probability (η close to zero). Table S4.1 presents the confidence intervals of the parameter estimates.

In Figure S4.1 we compare the estimate of the transmission rate β_1 for Sicilia to Lazio, a region with more typical results. The profiles for Sicilia support $\beta_1 \to 0$, which suggests a disease that is

Table S4.1: Region-specific MLEs for the stochastic Full Model

Region	Relative infectiousness θ	Relative reporting probability η
Lazio	0.74 (0.17, 1.00)	0.002 (0.000, 0.042)
Lombardia	0.54 (0.34, 1.00)	0.003 (0.000, 0.019)
Sardegna	1.00 (0.15, 1.00)	0.000 (0.000, 0.000)
Sicilia	1.00 (0.00, 1.00)	0.600 (0.000, 1.000)
Toscana	1.00 (0.01, 1.00)	0.035 (0.000, 1.000)
Umbria	1.00 (0.57, 1.00)	0.000 (0.000, 0.000)

not infectious at all and is simply dying out. Since this is not a plausible explanation of pertussis, the estimates for Sicilia is interprettedto be an artifact of the finte length of data available for Sicilia. We note that the best Waning Model fitted to Toscana data has a similar problem (but not the Leaky Model). We still continue to include the results for both Sicilia and Toscana in our aggregated profiles for completeness. Removing these do not qualitatively change the results.

S5 Reporting probability

In Trottier *et al.* (2006) the reporting probabilities of pertussis in industrialized countries were estimated to range from 3–12%. Sentinel surveillance in Italy have yielded estimates of vaccine-preventable disease prevalence (including pertussis) to be between 2.1–6.5 times higher than what was calculated using statutory notifications in northern Italy, and 9.1–15.8 times higher in southern Italy (Ciofi Degli Atti *et al.*, 2002). This indicates that the statutory notification rate is fairly low in Italy. The reporting probabilities calculated in this study were found to be between 1–3% for all the different regions of Italy, except in the case of Sicilia and the Waning Model for Toscana. For these exceptions, the best fit values for the observation probability were above 70%, due to the very low estimates of the transmission rate in these cases (discussed in Section S4). In the other cases, the estimates of the reporting probabilities may also be affected by our estimates of the basic reproduction number. This is discussed in the next section.

S6 Projections

We presented example simulations for the best model fit to Lazio in Figure 5. Here we used the birth and death rates from 2010–2012 from the Eurostat data. These were then fixed at the 2012 value for the remainder of the simulation (2013–2070). The population values from 2010–2012 were also taken from Eurostat and an annual rate of change of 0.4% was assumed from 2013–2070.

S7 Region-specific fits to the Restricted Models

Here we present the maximum likelihood estimates derived for each of the six regions of study. The estimates for the leakiness are shown in Table S7.2. For most regions, the confidence intervals for the leakiness parameter span almost the the entire allowable range of $(0, 1)$. The profiles for

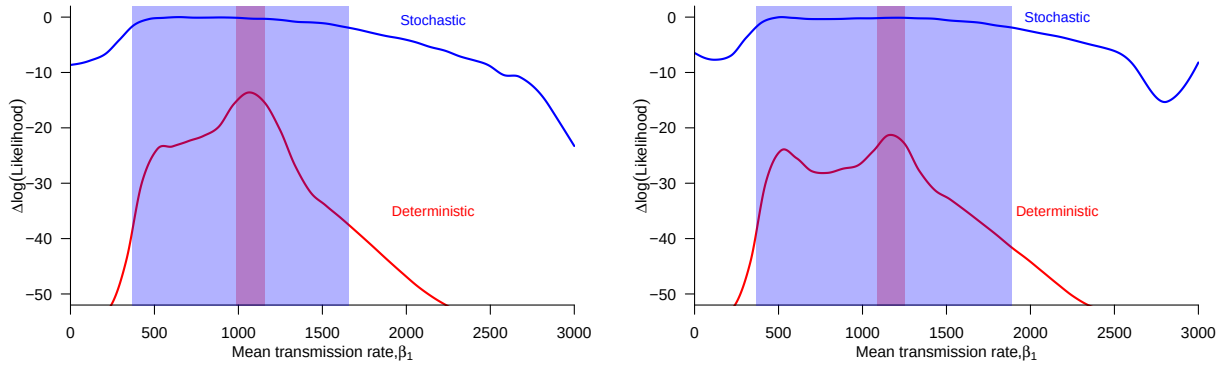

(A) Leaky Model of Lazio

(B) Waning Model of Lazio

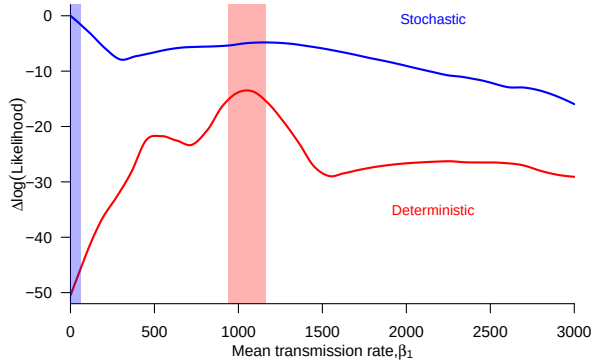

(C) Leaky Model of Sicilia

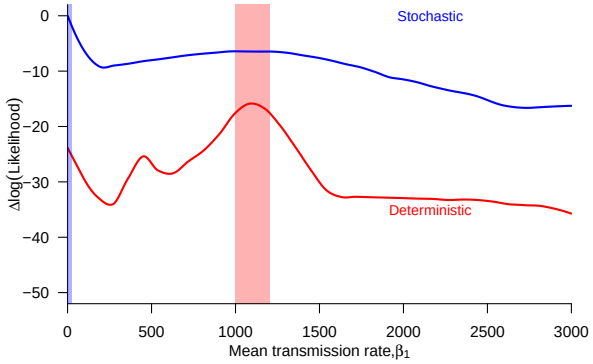

(D) Waning Model of Sicilia

Figure S4.1: Profiles over the transmission rate for the stochastic models fitted to data from the Lazio and Sicilia regions. This shows a maximum likelihood estimate of Sicilia that is highly inconsistent with other regions.

Lombardia displayed the most curvature at the MLEs and thus this region is associated with the smallest confidence intervals.

Table S7.2: Region-specific maximum likelihood estimates of the leakiness and mean transmission rate for the stochastic form of the Leaky Model

Region	Leakiness ε_L	Mean transmission rate β_1
Lazio	0.63 (0.07, 1.00)	650 (370, 1650)
Lombardia	0.17 (0.12, 0.25)	2000 (1450, 2730)
Sardegna	1.00 (0.05, 1.00)	530 (230, 2920)
Sicilia	0.02 (0.01, 0.70)	0 (0, 60)
Toscana	1.00 (0.02, 1.00)	490 (260, 3000)
Umbria	0.33 (0.10, 0.92)	1250 (600, 2830)

The estimates for the waning rate are shown in Table S7.3. In this case, three out of the six regions provide confidence intervals that are much smaller than the entire allowable range of $(0, 10)$. This suggests that the Waning Model may be less flexible than the Leaky Model for fitting the Italian data.

Table S7.3: Region-specific maximum likelihood estimates of the waning rate and mean transmission rate for the stochastic form of the Waning Model

Region	Waning rate α	Mean transmission rate β_1
Lazio	0.13 (0.05, 10)	520 (370, 1890)
Lombardia	0.10 (0.07, 0.16)	2060 (1570, 2720)
Sardegna	0.10 (0.02, 10)	1360 (250, 3000)
Sicilia	0.004 (0.001, 5.7)	0 (0, 30)
Toscana	0.008 (0.001, 10)	0 (0, 3000)
Umbria	0.96 (0, 10)	690 (160, 2070)

S8 Seasonal transmission

Due to the form of the seasonal transmission rate function (3), we could determine the timing of the peaks in transmission from the region-specific fits. This was found to be at $\varphi \approx 0.2$ of the year (mid-February) for most of the regions. We note that peaks in transmission should occur before peaks in incidence. Furthermore, since in our model, the disease is reported during the transition from infected to recovered (or effectively removed due to treatment or isolation), these peaks could be substantially separated by the mean incubation period of 8 days and infectious period of 14 days.

In Figure S8.2, we provide a profile of the seasonality parameters for the Leaky Model fit to Lombardia. The MLEs of the stochastic form of this model for the amplitude of seasonality and phase are $\beta_2 = 0.07(0.03, 0.11)$ and $\varphi = 0.22(0.12, 0.32)$ respectively.

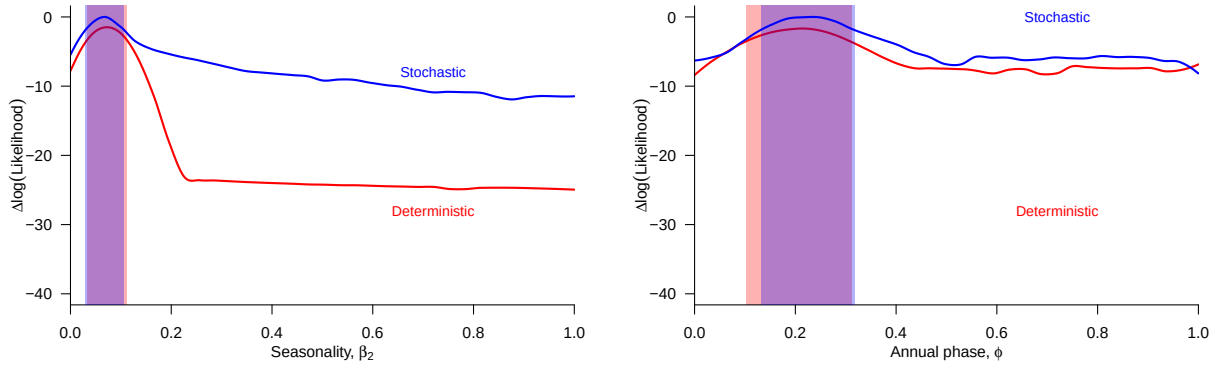

(A) Profile over the amplitude of seasonality β_2 for the Leaky Model

(B) Profile over annual phase φ for the Leaky Model

Figure S8.2: Profiles over the disease parameters for the stochastic models fitted to data from the Lombardia region.

We also tested the effect of using a more flexible seasonality function to our results. We re-fitted the Leaky Model of Lombardia using the following form of $\beta(t)$,

$$\beta(t) = \exp\Big(\sum_{i=1}^{6} b_i S_i(t)\Big), \tag{8}$$

where the S_i functions are periodic spline functions with a period of one. The parameters b_i were allowed to take any values in $\mathbb{R}$. This yields three extra parameters to the model. Since β_1 is no longer a parameter in such a model, the force of infection was changed from (2) to

$$\lambda(t) = \left(\frac{\beta(t)(I_1 + \theta I_2) + B\iota}{N(t)}\right) \Delta Q, \qquad \Delta Q \sim \text{Gamma}\left(\text{shape} = \frac{\Delta t}{\beta_{sd}^2}, \text{scale} = \frac{\beta_{sd}^2}{\Delta t}\right), \tag{9}$$

where $B = \int_0^1 \beta(t)dt$.

The Leaky Model using (8)–(9) was fitted to the Lombardia data and converged to the $\beta(t)$ function shown in Figure S8.3. Clearly the form $B(t)$ is different from a cosine curve. However, we note that the least-squares fit of a function of the form (3) to $B(t)$ has coefficients that are very similar to the values at the MLE of the original form of the Leaky Model. Similar results are found using the Waning Model. While this more flexible seasonality function provides slightly better likelihood values, the increase in number of parameters actually decreases the $\text{AIC}_c$of the new model. Furthermore, as shown in Figure S8.4, the estimates and confidence intervals of the relevant vaccine parameters do not change significantly with this new seasonality function.

S9 Sensitivity with respect to vaccine coverage assumption

Here we test the robustness of our results on the Restricted Models to changes in our assumptions of the unknown vaccination coverage from 1994–2000. We focus on the region of Lombardia because its likelihood profiles over the vaccine parameters display the most curvature compared to the other regions. In Figure S9.5, we demonstrate how the profiles change when the initial vaccine coverage

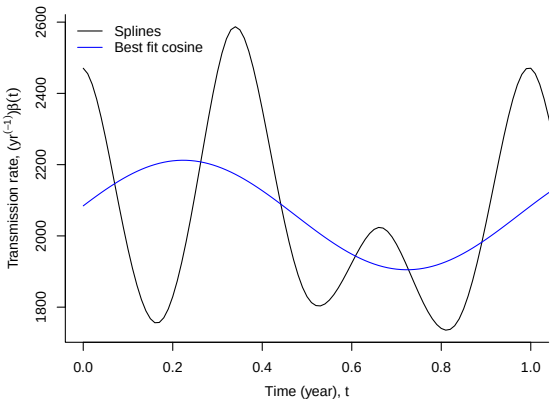

Figure S8.3: The seasonality function $B(t)$ of the form (8) at the MLE for the Leaky Model fit to Lombardia is shown in black. The curve of the form (3) fitted using least-squares to $B(t)$ is shown in blue. The fitted cosine curve has similar coefficients to those derived from the MLE of the original Leaky Model (with (3) as the seasonlity function).

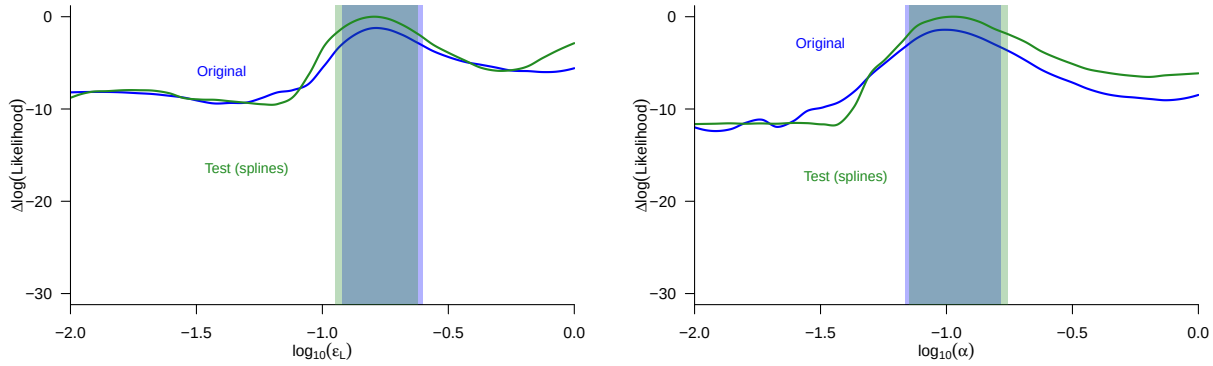

(A) Profile over leakiness ε_L for the Leaky Model

(B) Profile over waning rate α for the Waning Model

Figure S8.4: Profiles over the vaccine parameters for the stochastic models fitted to data from the Lombardia region. The profiles in green correspond to profiles using a seasonality function made up of six splines.

in 1994 is changed from 30% to 50%. In this case, the values with 95% confidence expand to include a disjoint interval that includes high levels vaccine failure ($\varepsilon_L = 1$ for the Leaky Model, and $\alpha = 10$ for the Waning Model). However the original MLEs and confidence intervals are still included in the confidence intervals of the new profiles, despite the large change in the vaccine coverage assumption. As noted in the main text, the fits to the data in Italy depend on factors that affect the vaccination level of the population, due to its effect on susceptibility of the population to the disease. When the initial vaccination coverage to 50%, more of the population was moved to the V class right from the beginning of the simulations. Thus to maintain the same number of susceptible individuals as in the original formulation, the model can compensate by making the vaccine less effective.

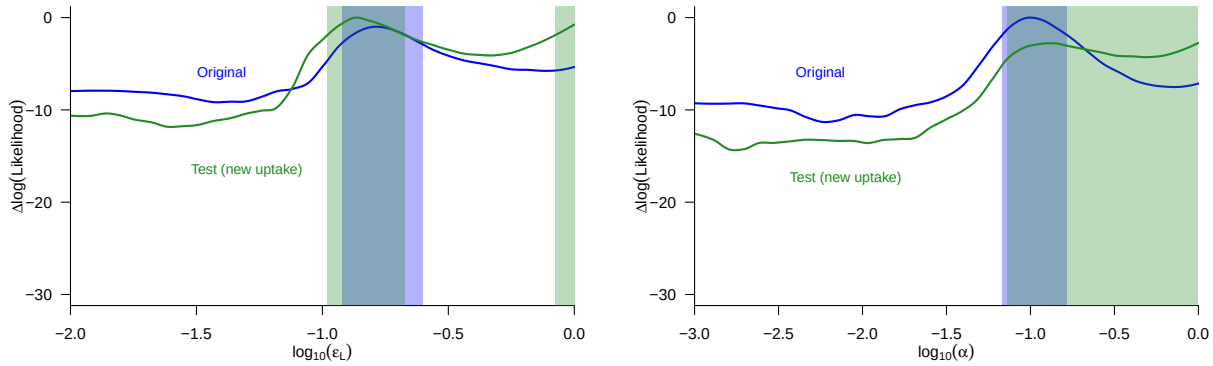

(A) Profile over leakiness ε_L for the Leaky Model

(B) Profile over waning rate α for the Waning Model

Figure S9.5: Profiles over the vaccine parameters for the stochastic models fitted to data from the Lombardia region. The profiles in green correspond to profiles where the initial vaccine coverage in 1994 is changed from 30% to 50%.

S10 Vaccine impact

Here we consider the effects of primary vaccine failure, leakiness, waning and relative infectiousness on transmission. Using the deterministic system of equations in (6) (with $K = 1$ and ignorning all superscripts for simplicity in notation) the disease-free equilibrium of this system $(V^*, S_1^*, E_1^*, I_1^*, S_2^*, E_2^*, I_2^*, R)^T$ is given by,

$$\begin{aligned} V^* &= \frac{p(1-\varepsilon_A)\mu}{\mu+\alpha}, \\ S_1^* &= 1-(1-\varepsilon_A)p, \\ S_2^* &= \frac{p(1-\varepsilon_A)\alpha}{\mu+\alpha}, \\ E_1^* &= I_1^* = E_2^* = I_2^* = R^* = 0. \end{aligned} \tag{10}$$

Let $\beta(t) = \beta$ (a constant) and define $X = (E_1, I_1, E_2, I_2)^T$. Linearizing about the disease free equilibrium yields,

$$\frac{dX}{dt} = (\mathcal{F} - \mathcal{V})X, \tag{11}$$

where

$$\mathcal{F} = \begin{pmatrix} 0 & S_1^* & 0 & \theta S_1^* \\ 0 & 0 & 0 & 0 \\ 0 & S_2^* + \varepsilon_L V^* & 0 & \theta(S_2^* + \varepsilon_L V^*) \\ 0 & 0 & 0 & 0 \end{pmatrix}, \qquad \mathcal{V} = \begin{pmatrix} \sigma + \mu & 0 & 0 & 0 \\ -\sigma & \gamma + \mu & 0 & 0 \\ 0 & 0 & \sigma + \mu & 0 \\ 0 & 0 & -\sigma & \gamma + \mu \end{pmatrix}. \quad (12)$$

To derive the basic reproduction number of this system, we first derive the next generation matrix $K = \mathcal{F}\mathcal{V}^{-1}$. The sole non-zero eigenvalue of this matrix yields the expression for the basic reproduction number R_p,

$$R_p = \frac{\beta\sigma}{(\mu+\sigma)(\mu+\gamma)}\big[S_1^* + \theta(S_2^* + \varepsilon_L V^*\big] \quad (13)$$

If we use the previously introduced Magpantay *et al.* (2014) notation $\varepsilon_W = \frac{\alpha}{\mu+\alpha}$, then we derive,

$$R_p = R_0(1 - \varphi p), \quad (14)$$

where $R_0 = \frac{\beta\sigma}{(\mu+\sigma)(\mu+\gamma)}$ and the vaccine impact is given by,

$$\varphi = (1 - \varepsilon_A)\big[(1-\theta) + \theta(1-\varepsilon_L)(1-\varepsilon_W)\big]. \quad (15)$$

If, as in the main text, we set the primary vaccine failure $\varepsilon_A = 0$, then this expression simplifies to,

$$\varphi = (1-\theta) + \theta(1-\varepsilon_L)(1-\varepsilon_W). \quad (16)$$

One can calculate the critical vaccination coverage, the minimum fraction of the population that needs to be vaccinated to obtain asymptotic eradication of the disease, by setting $R_0 \leq 1$. This yields,

$$p \leq p_c(\text{the critical vaccination coverage}) := \frac{1}{\varphi}\big[1 - \frac{1}{R_0}\big].$$

Since the critical vaccination coverage can be considered a measure of the total reduction in transmission (due to both reduction in susceptibility of vaccinated individuals, and reduction in their transmission potential if they get infected), we can look at the vaccine impact φ as a measure of the reduction in overall transmission due to vaccination.

S11 Mean age at first infection of naïve individuals

The values in Table 7 were calculated by taking the full collection of points and likelihoods measured for Lazio (including the initial run and all profiles) and discarding those wherein the relevant vaccine parameters (leakiness for the Leaky Models and waning rate for the Waning Model) do not fall within the confidence intervals in Table 7. We then used the likelihoods to take 50 samples from these points. At each sample, we found the filter means of the states from 1994–2070 (filtered through data consisting of the original data from 1994–2009 augmented by NA values from 2010–2070, each NA value was assumed to have probability of one). The collection of filter means were then used to derive the mean age at first infection of naïve individuals, as well as the 2.5% and 97.5% quantiles.

S12 Basic reproduction number for systems with and without age-structure

The basic reproduction number is an important concept in epidemiology and represents the expected number of secondary cases resulting from the introduction of one infected case in a wholly susceptible population. This can be derived from linearization of the systems about the disease-free equilibrium (van den Driessche & Watmough, 2008). While a particular disease is often associated with a range of basic reproduction number values, this number actually also depends on the model that is being used to represent the disease dynamics. In this section we discuss how an estimate of basic reproduction number varies when we use a (1) homogenous model and (2) an age-structured model with two age classes to model a disease at steady state.

The system of equations for the age-structured model is given by,

$$\begin{aligned}
\frac{dS_1}{dt} &= \mu - \lambda_1 S_1 - \nu S_1 - \mu S_1, \\
\frac{dI_1}{dt} &= \lambda S_1 - \gamma I_1 - \nu I_1 - \mu I_1, \\
\frac{dR_1}{dt} &= \gamma I_1 - \nu R_1 - \mu R_1, \\
\frac{dS_2}{dt} &= \nu S_1 - \lambda_2 S_2 - \mu S_2, \\
\frac{dI_2}{dt} &= \nu I_1 + \lambda_2 S_2 - \gamma I_2 - \mu I_2, \\
\frac{dR_2}{dt} &= \nu R_1 + \gamma I_2 - \mu R_2.
\end{aligned} \tag{17}$$

Here,

$$\begin{aligned}
\lambda_1 &= \beta_{11} I_1 + \beta_{12} I_2, \\
\lambda_2 &= \beta_{21} I_1 + \beta_{22} I_2.
\end{aligned} \tag{18}$$

and

$$\begin{bmatrix} \beta_{11} & \beta_{12} \\ \beta_{21} & \beta_{22} \end{bmatrix} = \beta \begin{bmatrix} \varphi & \chi \\ \chi & 1 \end{bmatrix} \tag{19}$$

where $\varphi > 1$ and $\chi \in (0, 1]$ to reflect higher than average contacts between children and lower contacts between adults and children.

In Figure S12.6 we present the basic reproduction number of the age-structured model compared to that of a homogenous model with the same mean age at first infection. All of these values were calculated numerically with all model parameter values fixed except for the transmission rate β_1. We see that in a homogenous approximation of an age-structured system, estimates of the basic reproduction number can be much higher than the reproduction number associated with the age-structured system. Depending on the value of φ, this could also be lower. Thus we see that fitting a homogenous model to data that may have been generated from age-structured data can affect the estimates of R_0. For this reason, we do not focus on the estimates of R_0 in this project. Instead we look at the mean age at first infection which is more consistent across regions. Furthermore, the high estimates of R_0 that we measured due to our use of a homogenous model may be trading off with the low reporting rates that we observed in Section S5. Our assumption that wP-induced

immunity can be considered the same as infection-derived immunity may also play a part in our wide range of estimates for the transmission rate β_1 and therefore R_0.

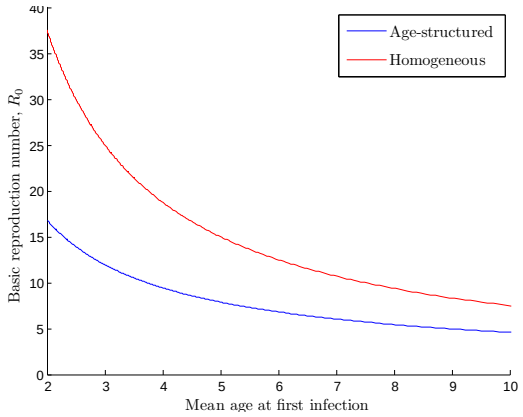

Figure S12.6: Comparison of the basic reproduction number for homogenous and age-structured models at the same values of the steady state mean age at first infection for $\varphi = 3$ and $\chi = 1$. In this case, the transmission between children is three times larger than transmission between all other types of transmissions (between adults, between an adult and a child).

REFERENCES

Burnham, K. P. and Anderson, D. R. (2002). *Model Selection and Multimodel Inference: A Practical Information-Theoretic Approach (2nd ed.)*. Springer-Verlag New York.

Ciofi Degli Atti, M., Salmaso, S., Bella, A., Arigliani, R., Gangemi, M., Chiamenti, G., Brusoni, G., Tozzi, A. E. and Pediatric Sentinel Surveillance Study Group (2002). Pediatric sentinel surveillance of vaccine-preventable diseases in Italy. *Pediatric Infectious Disease Journal* **21(8)**, 763–768.

European Commission (2014). Regional Statistics. URL `http://ec.europa.eu/eurostat/data/database`. (accessed 01-February-2014).

He, D., Ionides, E. L. and King, A. A. (2010). Plug-and-play inference for disease dynamics: measles in large and small populations as a case study. *Journal of The Royal Society Interface* **7**, 271–283. doi: 10.1098/rsif.2009.0151.

Magpantay, F. M. G., Riolo, M. A., Domenech de Cellès, M., King, A. A. and Rohani, P. (2014). Epidemiological consequences of imperfect vaccines for immunizing infections. *SIAM Journal on Applied Mathematics* **74(6)**, 1810–1830. doi: 10.1137/140956695.

Ministero della Salute (2014). Coperture vaccinali. URL `http://www.salute.gov.it/portale/temi/p2_6.jsp?id=811&area=Malattie%20infettive&menu=vaccinazioni`. (accessed 8 January 2014).

Trottier, H., Carabin, H. and Philippe, P. (2006). Proportion des déclarations de cas de rouge ole, de coqueluche, de rubéole et d'oreillons aux systémes de surveillance. évaluation des études pour les pays industrialisés. *Rev Epidemiol Sante Publique* **54**, 27–39.

van den Driessche, P. and Watmough, J. (2008). Further notes on the basic reproduction number. In *Mathematical Epidemiology* (eds. F. Brauer, P. van den Driessche and J. Wu), chap. 6, pp. 159–178. Springer.